



# Management of MRI-Detected Benign Internal Mammary Lymph Nodes

Gozde Gunes<sup>1</sup> Priscila Crivellaro<sup>2</sup> Derek Muradali<sup>2</sup>

<sup>1</sup>Department of Radiology, Baskent University Hospital, Çankaya/Ankara, Turkey

<sup>2</sup>Department of Medical Imaging, University of Toronto, Toronto, Ontario, Canada

Address for correspondence Gozde Gunes, MD, Department of Radiology, Baskent University Hospital, Yukarı Bahçelievler, Mareşal Fevzi Çakmak Cd. No:45, 06490 Çankaya/Ankara, Turkey (e-mail: gunesgozde@gmail.com).

Indian J Radiol Imaging 2022;32:197–204.

## Abstract

**Introduction** In this retrospective study, we aimed to evaluate benign internal mammary lymph nodes (IMLNs) in terms of frequency, number, size, long axis/short axis (L/S) ratio, intercostal location, presence of fatty hilum, and stability using breast magnetic resonance imaging (MRI) and discuss the findings by reviewing existing literature.

**Methods** This single-center study consisted of 130 women between the ages of 24 and 76 years, who had at least two breast MRI examinations in our institution, with the latest exam performed between January 1, 2019 and November 1, 2019, were eligible for the study. MRIs of the study group were independently reviewed by two radiologists.

**Results** IMLN was detected in 31.1% of the 427 MRIs, with a total number of 256 nodes. The most common indication for breast MRI was high-risk screening (66.2%). The median number of nodes per patient was 1 (range: 1–6). The median follow-up time was 19.5 months (range: 6–141 months). None of these benign nodes showed significant interval growth. Mean L/R ratio of the nodes was 1.9. One hundred and four nodes ( $n = 104$ , 40.6%) had a L/S ratio less than 2 and 43.2% ( $n = 45$ ) of the nodes with a L/S ratio less than 2, had a long axis measuring less than or equal to 3mm. IMLN of patients with breast implants had the largest mean long axis. The fatty hilum was identified in 34.3% ( $n = 68$ ) of the 256 nodes. The size of the lymph nodes where fatty hilum was visualized was significantly larger than the ones where fatty hilum was not visualized ( $p < 0.001$ ). Fatty hilum could be visualized in only 2.7% of the nodes with a long axis smaller than 3 mm.

**Conclusion** IMLN is a frequent finding on breast MRI. We have shown that benign IMLNs might be large sized in specific cases like patients with breast implants. When small sized ( $\leq 3$ mm), they are more likely to be rounded (L/S ratio  $< 2$ ). The fatty hilum that is a feature of benignity might not be visualized in nodes less than or equal to 3mm.

## Keywords

- ▶ screening
- ▶ internal mammary lymph node
- ▶ MRI
- ▶ breast cancer
- ▶ high risk

published online  
July 13, 2022

DOI <https://doi.org/10.1055/s-0042-1750180>.  
ISSN 0971-3026.

© 2022. Indian Radiological Association. All rights reserved.  
This is an open access article published by Thieme under the terms of the Creative Commons Attribution-NonDerivative-NonCommercial-License, permitting copying and reproduction so long as the original work is given appropriate credit. Contents may not be used for commercial purposes, or adapted, remixed, transformed or built upon. (<https://creativecommons.org/licenses/by-nc-nd/4.0/>)  
Thieme Medical and Scientific Publishers Pvt. Ltd., A-12, 2nd Floor, Sector 2, Noida-201301 UP, India

## Introduction

With the increased number of daily breast magnetic resonance imaging (MRI) examinations performed with modern scanners that have the capability to produce thin slice, high-resolution images, more and more incidental (liver cysts, thyroid nodules) or benign findings are being documented.<sup>1</sup> One of these findings are internal mammary lymph nodes (IMLNs). Unlike axillary lymph nodes, no current guideline or imaging criteria exist for characterizing these nodes that are often benign in the absence of neoplastic disease of the breast.

High-risk screening is the most common indication for breast MRI. Breast cancer risk of women have been classified as average, intermediate, or high, based on genetic profile, personal history of high-risk breast lesions or breast cancer, history of chest wall radiation, etc.<sup>2</sup> Being the most common nonskin cancer among women, screening for breast cancer for high-risk patients has been emphasized in the latest years. With the consensus based on scientific data showing different risks among different risk groups, screening regimens have become tailored to the individual patient with the guidance of national screening programs. The Ontario Breast Screening Program (OBSP) recommends screening women between ages of 30 and 69 years who are confirmed to be at high risk of developing breast cancer, once a year with a mammogram and breast MRI (or screening breast ultrasound if MRI is not medically appropriate).<sup>3</sup> The American Cancer Society, National Comprehensive Cancer Network, and American College of Radiology recommend breast MRI for screening as an adjunct to screening mammography for high-risk women.<sup>4,5</sup> Previous studies showed that breast MRI is superior to breast ultrasound and mammography with a sensitivity ranging from 64 to 100%.<sup>6</sup>

In addition to screening purposes, there are other indications for breast MRI, such as further evaluation of findings that are initially detected on mammogram and/or ultrasound or evaluation of breast implants.

Compared with IMLN, axillary lymph nodes have been much more analyzed throughout the years since the lymphatic drainage of the breast is mainly managed by axillary lymph chain and axillary region is the first route for systemic spread of breast carcinoma.

For characterizing malignant axillary lymph nodes, ultrasound was found to be 94% sensitive and 72% specific. Sonographic criteria were based on size, long axis/short axis (L/S) ratio, thickness of the cortex, and morphologic features (absence or presence of fatty hilum).<sup>7</sup> Normal hilar fat has increased signal intensity on nonfat-saturation MRI sequences and decreased signal intensity on fat-saturation MRI sequences (→ Fig. 1). Loss of hilar fat by the invasion of malignant cells is also a good predictor of malignancy. Another useful criterion is L/S ratio that has been shown to be 97% specific for malignancy with values less than 2.<sup>8</sup> Using these features, the suspicious axillary node could be detected with a high sensitivity and specificity by ultrasound, computed tomography, or MRI. In addition to these, since easily approached, ultrasound-guided fine-needle aspiration (FNA)



**Fig. 1** Axial plane, postcontrast magnetic resonance image of a right-sided internal mammary lymph node in the second intercostal space, which measures 8 × 3 mm. The low intensity fatty hilum is clearly seen (arrow).

for axillary lymph nodes is often and easily performed during daily practice. Apart from imaging, axillary lymphadenectomy or sentinel lymph node biopsy is also standard procedure for breast cancer patients. Unlike axillary nodes, detecting and characterizing nodes of internal mammary chain, which is the second main drainage pathway of the breast, are much more difficult. The internal mammary lymphatic chain is located just anterior to the extra pleural space and within the intercostal space that contains internal mammary artery, internal mammary vein, internal mammary lymphatic chain, and fat. The internal mammary vessels run through this space along the first intercostal space to the sixth, either medial or lateral to nodes.

Except some medical facilities, routine IMLN imaging or FNA is not part of the diagnostic process. There are few studies in this subject such as Dogan et al's that included preoperative and pretreatment ultrasound of 595 patients and found 58 suspicious IMLNs, which were confirmed by sentinel lymph node dissection and multislice imaging modalities after neoadjuvant chemotherapy.<sup>9</sup>

We know that tumoral spread to axillary or internal mammary chain upgrades the staging that alters the treatment and survival.<sup>10</sup> The updated National Comprehensive Cancer Network (NCCN) Breast Cancer Clinical Practice Guidelines in 2016 recommends IMLN irradiation for patients with more than or equal to 4 positive axillary nodes, and strongly considers IMLN irradiation for patients with 1 to 3 positive axillary lymph nodes.<sup>11</sup>

Today, due to increased number of breast MRIs (mostly due to high-risk screening) more and more IMLNs, most of which have totally benign features, are being identified and reported. This overcalling might lead to unnecessary imaging follow-ups that mean anxiety for the patient, confusion for the clinician, and waste of sources.

In this retrospective study, we aimed to evaluate benign IMLNs in terms of frequency, number, size, L/S ratio, intercostal location, presence of fatty hilum, and stability using breast MRI and discuss the findings by reviewing existing literature.

## Materials and Methods

### Patient Selection

Our retrospective single-center study finally consisted of 130 women between the ages of 24 and 76 who had breast MRI examination in our institution between January 1, 2019 and November 1, 2019. The study was approved by the Unity Health Toronto Research Ethics Board. Patient history was obtained from review of the electronic medical records of our institution. The indications for breast MRI were high-risk screening, family history of breast cancer (intermediate risk), referral from mammography or breast ultrasound, dense breasts, implant imaging, and discordant biopsy results. High risk is defined by the OBSP as “women between the age of 30 and 69 who meet one of the following criteria: **a.** Known to be a carrier of a gene mutation (e.g., BRCA1, BRCA2). **b.** First degree relative of a carrier of a gene mutation (e.g., BRCA1, BRCA2), has previously had genetic counselling, and has declined genetic testing. **c.** Previously assessed by a genetic clinic (using the IBIS or BOADICEA risk assessment tools) as having a more than 25% lifetime risk of breast cancer on basis of family history. **d.** Received chest radiation (not chest X-ray) before the age of 30 and at least 8 years previously.”

We listed all the patients who had breast MRI during the defined period, with at least one prior MRI. A total of 854 cases were found. We excluded 427 of them based on our exclusion criteria that are as follows:

- No breast MRI follow-ups ( $n = 185$ )
- History of breast carcinoma/recently diagnosed breast carcinoma ( $n = 225$ )
- History of recently diagnosed carcinoma other than breast ( $n = 5$ )
- History of chest radiotherapy ( $n = 2$ )
- Suboptimal/low-quality MRI (lack of contrast, motion artifact, missing sequence) ( $n = 10$ )

After excluding 427 cases, 427 MRIs were left for the study. After carefully evaluating the remaining MRIs, 140 cases were found to be positive for IMLN. Duplicated cases ( $n = 10$ ) who had more than one breast MRI in the study period were counted as one with the latest MRI exam taken into account. Overall, 130 patients were eligible out of 417 patients without malignancy.

### Imaging Technique and Analysis

Two MRI scanners (1.5T and 3T) were used with standardized imaging protocols. The 1.5T system (Ingenia CX; Phillips) consisted of axial bilateral three-dimensional T2 7-channel images (repetition time msec/echo time msec, 1300/167; flip angle: 90 degrees) with a  $360 \times 357$  acquisition matrix, axial bilateral three-dimensional T2 SPAIR 7-channel (using identical parameters), and axial diffusion-weighted images (B val-

ues: 0 and 1,000; repetition time msec/echo time msec, 11,184/94; flip angle: 90 degrees) with a  $112 \times 135$  acquisition matrix. Dynamic contrast-enhanced THRIVE images were then performed (repetition time msec/echo time msec, 5.4/2.7; flip angle: 90 degrees) using a  $352 \times 425$  acquisition matrix. The 3T system (Skyra; Siemens Healthcare) consisted of axial bilateral 2 mm STIR images (repetition time msec/echo time msec, 5,630/95; flip angle: 80 degrees) using a  $320 \times 240$  acquisition matrix, axial bilateral T1 three-dimensional images (repetition time msec/echo time msec, 6.10/2.21; flip angle: 20 degrees) degrees using a  $384 \times 365$  acquisition matrix, and axial bilateral diffusion images (B values: 0 and 1000; repetition time msec/echo time msec, 5,800/62; flip angle: 90 degrees) using a  $200 \times 108$  acquisition matrix. Dynamic contrast-enhanced VIBE images were then performed (repetition time msec/echo time msec,  $4.10 \times 1.99$ ; flip angle: 10 degrees).

Dynamic contrast-enhanced breast MRI was performed with a bolus injection of 0.1 mmol per kilogram of body weight of gadobenate dimeglumine (529 mg/mL) (Multihance; Bracco). Double-breast surface coils were used, dS Breast 7ch 1.5 T in vivo for the 1.5 T system and 2/10/16-Channel Sentinelle Breast Coil for the 3 T system.

MRIs of the study group, which were obtained from our picture archiving and communication systems, were retrospectively and independently reviewed at a workstation by two radiologists, one of which is a breast radiologist with more than 20 years of experience and the other one, a breast imaging fellow, who were blinded to the complete patient history. Dynamic contrast-enhanced sequences as well as T2-weighted sequence on the axial plane were mainly used for the evaluation of the nodes. Only IMLN-positive cases were evaluated further in terms of number, size, location (regarding intercostal space), presence or absence of fatty hilum as well as accompanying breast lesions. The size of the node was measured on the axial plane involving long and short axis. L/S ratio was then calculated for each case. For cases with more than one node, each node was measured separately. For each case, each node was compared with the oldest available study. We defined growth as more than 2mm difference in the short axis measurement between two MRI exam. In case of discordance between readers, a consensus was made by a third breast radiologist with 20 years of experience of breast imaging.

### Statistical Analyses

Data analysis was performed using IBM SPSS Statistics version 17.0 software (IBM Corporation, Armonk, New York, United States). Kolmogorov–Smirnov test was used to investigate the normal distribution assumption. Categorical data were expressed as numbers ( $n$ ) and percentage (%) while quantitative data were given as mean  $\pm$  standard deviation and median (min–max). While the differences in node sizes and L/S ratios regarding for presence of fatty hilum were compared by Mann–Whitney U test, Kruskal–Wallis test was applied for the comparisons among MRI indications. A  $p$ -value less than 0.05 was considered statistically significant.

**Table 1** Demographic and clinical characteristics of the cases

	<i>n</i> = 130
Age (y), mean $\pm$ SD	48.7 $\pm$ 10.7
Range of ages (y)	24–76
Indication	
High-risk screening	86 (66.2%)
Mammography referral	17 (13.0%)
Family history of breast cancer (intermediate risk)	7 (5.4%)
Implant imaging	7 (5.4%)
Dense breasts	6 (4.6%)
US referral	5 (3.9%)
Discordant biopsy results	2 (1.5%)
Total number of IMLN per patient, <i>median (min–max)</i>	1 (1–6)
Side	
Right	40 (30.8%)
Left	37 (28.5%)
Bilateral	53 (40.7%)
Fatty hilum	
Absent (not visualized)	62 (47.7%)
Present	68 (52.3%)
Follow-up time (mo), <i>median (min–max)</i>	19.5 (6–141)

Abbreviations: IMLN, internal mammary lymph node; min, minimum; max, maximum; SD, standard deviation.

## Results

Out of the total 854 breast MRIs, 427 cases were excluded based on our exclusion criteria. Out of the 427 cases, 140 had at least a single IMLN. Ten studies were found to be duplicated, therefore excluded, leaving 130 cases finally eligible for the study. Overall, positivity rate for IMLN was found to be 31.1% among 417 breast MRI exams analyzed.

The most common indication for breast MRI was high-risk patient screening with 86 patients (66.2%), followed by mammography referral, family history of breast cancer (intermediate risk), breast implant imaging, dense breasts,

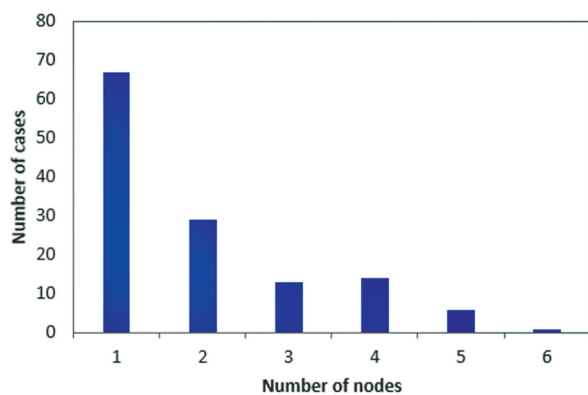


**Fig. 2** Each bar on the x-axis indicates the number of nodes. The frequency (a.k.a. the number of cases) levels regarding for each bar are represented on the y-axis.

ultrasound referral, and discordant biopsy results (**Table 1**). The ages of the patients were between 24 and 76 with the median age of 48.7  $\pm$  10.7 years. The median follow-up period was 19.5 months, ranging between 6 and 141 months. All the IMLNs were stable based on our growth criterion. A total number of 256 nodes were identified among 130 patients. The median number of nodes per patient was 1 (range: 1–6, **Fig. 2**), as 51.5% (*n* = 67) of the cases had only a single node. The number of patients with total number of 1, 2, 3, 4, 5, and 6 nodes were 67, 30, 12, 14, 6, and 1, respectively. Lymph nodes were only right sided in 30.8% of cases (*n* = 40), only left-sided in 28.5% (*n* = 37), and bilateral in 40.7% (*n* = 53) of cases. **Table 2** summarizes the frequency distribution of the location of the nodes with respect to intercostal space. Most involved intercostal space was the second, followed by the third and first.

Descriptive statistics for node sizes are given in **Table 3**. Regardless of the fatty hilum, mean L/S ratio among 256 nodes was 1.90. L/S ratio of one hundred and four nodes (*n* = 104, 40.6%) was less than 2 and 21 nodes had L/S ratio equal to 1. Out of these 21 round nodes, thirteen measured 1  $\times$  1 mm, three measured 2  $\times$  2 mm, four measured 3  $\times$  3 mm, and one measured 4  $\times$  4 mm. We had a number of 74 nodes with L/S ratio of 1.5 and 30 nodes with L/S ratio ranging between 1.5 and 2. Overall, 43.2% (*n* = 45) of the nodes with L/S ratio less than 2 had a long axis measuring less than or equal to 3mm.

In **Table 4**, we see the mean node size and mean L/S ratio of different indication groups. Patients with implants had the

**Table 2** Frequency distribution of intercostal spaces ( $n = 256$ )

	<i>n</i>	%
1st	43	16.7
2nd	117	45.7
3rd	75	29.2
4th	14	5.4
5th	5	1.9
6th	2	0.7

largest nodes compared with nodes of other indication groups. Mean long axis of the largest node of each patient with implant was  $5.43 \pm 2.37$  (2–8) with a mean L/S ratio of  $1.72 \pm 0.17$ .

The number of nodes with positive fatty hilum was 88 (34.3%), whereas the number of nodes without fatty hilum was 168 (65.7%). At least one node had a fatty hilum in 52.3% ( $n = 68$ ) of the patients. When each node was evaluated separately in terms of fatty hilum and L/S ratio, while nodes with positive fatty hilum had a mean L/S ratio of  $1.84 \pm 0.53$ , the mean L/S ratio of nodes without fatty hilum was

$2.03 \pm 0.67$ . No statistically significant correlation was found between fatty hilum and L/S ratio ( $p = 0.062$ ). The size of the lymph nodes where fatty hilum was visualized was significantly larger than the ones where fatty hilum was not visualized ( $p < 0.001$ ) (►Fig. 3). We could not detect fatty hilum in any of the nodes measuring  $1 \times 1$  mm ( $n = 14$ ) and in 96.5% ( $n = 56$ ) of the nodes measuring  $2 \times 1$  mm ( $n = 56$ )/  $2 \times 2$  mm ( $n = 2$ ).

Ipsilateral breast lesions and history of ipsilateral breast biopsy/surgery are summarized in ►Table 5. Ten percent (10%) of the patients had an ipsilateral intramammary lymph node and 3.8% had an ipsilateral prominent axillary lymph node (cortical thickness greater than 3mm), all of which were revealed to be benign either by follow-up or biopsy. Other than these findings, 20 solid masses were identified among 130 cases, of which 15 had been biopsied with results of fibroadenoma ( $n = 10$ ), tubular adenoma ( $n = 1$ ), and papilloma ( $n = 4$ ). Nonbiopsied masses were regarded as benign due to lack of interval change on follow-up for at least 2 years.

Cases that had a history of ipsilateral breast intervention (32.3%,  $n = 42$ ) are as follows: lumpectomy/mass excision ( $n = 10$ ), ultrasound-guided biopsy ( $n = 20$ ), stereotactic guided biopsy ( $n = 4$ ), and MRI-guided biopsy ( $n = 10$ ). One

**Table 3** Descriptive statistics for node sizes

Nodes overall, mean $\pm$ SD (min–max)	<i>n</i> = 256
Long axis (mm)	$3.93 \pm 1.9$ (1–12)
L/S ratio	$1.90 \pm 0.59$ (1–5)
The largest node of each case, mean $\pm$ SD (min–max)	<i>n</i> = 130
Long axis (mm)	$4.57 \pm 1.92$ (1–12)
L/S ratio	$1.92 \pm 0.53$ (1.0–5.0)
The largest node of fatty hilum positive cases, mean $\pm$ SD (min–max)	<i>n</i> = 68
Long axis (mm)	$5.38 \pm 1.72$ (2–10)
L/S ratio	$2.03 \pm 0.60$ (1–5)

Abbreviations: L/S ratio, long axis/ short axis ratio; max, maximum; min, minimum; SD, standard deviation.

**Table 4** The comparisons of node sizes (mm) among indications

	Mean long axis (mm)	L/S ratio
Implant Imaging	$5.43 \pm 2.37$ (2–8)	$1.72 \pm 0.17$ (1.5–2.0)
US referral	$5.40 \pm 2.61$ (3–9)	$1.93 \pm 0.37$ (1.5–2.5)
High-risk screening	$4.70 \pm 1.95$ (1–12)	$1.99 \pm 0.58$ (1.0–5.0)
Family history of breast cancer (intermediate risk)	$4.14 \pm 2.11$ (1–8)	$1.82 \pm 0.62$ (1.0–3.0)
Mammography referral	$3.94 \pm 1.25$ (2–6)	$1.84 \pm 0.39$ (1.0–2.5)
Dense breasts	$3.67 \pm 1.75$ (1–6)	$1.59 \pm 0.35$ (1.0–2.0)
Discordant biopsy results	$3.50 \pm 0.71$ (3–4)	$1.56 \pm 0.08$ (1.5–1.6)
<i>p</i> -Value <sup>a</sup>	0.411	0.231

Abbreviations: L/S, long/short axis; SD, standard deviation; US, ultrasound.

Data were shown as mean  $\pm$  SD (min–max),

<sup>a</sup>Kruskal–Wallis test. L/S ratio.

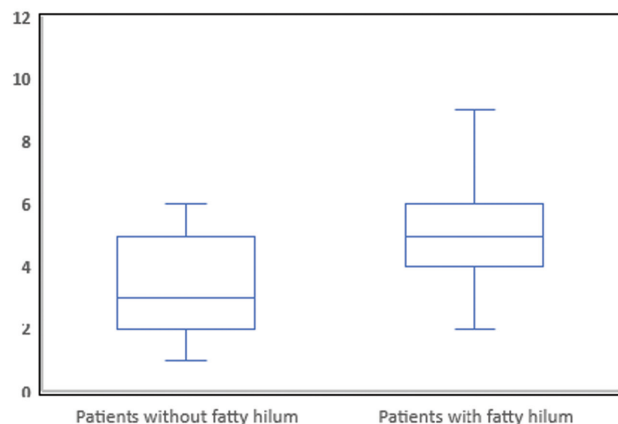


**Fig. 3** Comparison of the long axis size of nodes in patients with and without fatty hilum. The y-axis indicates the size of the long axis. The horizontal lines in the middle of each box indicate the median, while the top and bottom borders of the box mark the 25th and 75th percentiles, respectively. The whiskers above and below the box mark the maximum and minimum levels of node sizes.

of the patients had both mammography-guided and MRI-guided biopsy and one had both ultrasound-guided biopsy and surgery.

Nineteen patients had bilateral breast implants. Six of them had implant rupture (4 extracapsular, 2 intracapsular).

## Discussion

As the number of breast MRI examinations have increased in the last decade, mostly due to high-risk screening, we are

**Table 5** Frequency distributions of ipsilateral breast mass lesions and biopsy/surgery

	n = 130
<b>Breast mass lesions (ipsilateral)</b>	
Papilloma	4 (3.1%)
Fibroadenoma	10 (7.7%)
Reactive intramammary lymph node (ipsilateral)	13 (10.0%)
Prominent axillary lymph node (ipsilateral)	5 (3.8%)
Cyst	14 (10.8%)
Tubular adenoma	1 (0.8%)
Solid mass (not biopsied)	5 (3.8%)
None	80 (61.5%)
<b>History of breast biopsy/ surgery (ipsilateral)</b>	
MR-guided biopsy	10 (7.7%)
US-guided biopsy	20 (15.4%)
Mammography-guided biopsy	4 (3.1%)
Surgery	10 (7.7%)
None	88 (67.7%)

Abbreviations: MR, magnetic resonance; US, ultrasound.

more challenged by incidental findings such as benign axillary or IMLNs.<sup>12</sup> Unlike axillary nodes that are much more easily identified given the superficial location and relatively larger size, IMLNs are more difficult to identify, hence might be overlooked. When identified, radiologists face this uncertainty of how to approach as we lack a certain guideline for classifying them. While overcalling might cause anxiety, confusion, waste of sources, underdiagnosing might lead to staging errors, therefore inadequate treatment. As we know lymphatic spread is the most common route of initial metastasis for carcinomas that impacts disease stage, prognosis, and survival, it is essential to select the suspicious nodes.<sup>13–15</sup> In our study, we have detected a total of 256 IMLNs among 427 breast MRIs evaluated. We have excluded 185 cases as they lacked follow-up MRI.

In 2015, Mack et al published a retrospective study including breast MRIs of 108 asymptomatic high-risk women.<sup>16</sup> Their study had this limitation of involving only single MRI for assessing IMLNs rather than comparing with priors to ensure benignity and lack of interval change.

IMLNs were described as a common finding of high-risk screening with being positive in 50 of the 108 cases (46%) with the average size of 4.50 mm (range: 2–9 ± 1.59 mm) in the greatest diameter. In our study, IMLN was found in 130 out of the 417 patients (31.1%) with the average long axis diameter of 3.93 mm (range: 1–12 ± 1.9).

Mack et al found IMLNs most frequently in the second intercostal space followed by the third intercostal space. All the 26 malignant IMLNs were found within the first three intercostal space by Sachdev et al.<sup>17</sup> Similarly, Wang et al showed that the second and first intercostal spaces were most likely to be involved by malignant nodes.<sup>18</sup> We also detected IMLN mostly in the second intercostal space followed by the third intercostal space. The evaluation of the narrow first intercostal space might be limited in some cases. So, whether malignant or not, IMLNs have been mostly found in the first three intercostal spaces.

Mean L/S ratio was found to be 1.9 (range: 1–5 ± 0.59) in our study. Previous studies have shown that for axillary, cervical, and supraclavicular lymph nodes, L/S ratio less than 2 is a feature of malignancy.<sup>19–22</sup> In our study, no cutoff point for the L/S ratio could be given since a comparison group was lacking. About 40.6% of the nodes in our study had L/S ratio less than 2 and of these nodes, 43.2% had a long axis measuring less than or equal to 3mm. We believe for small-sized benign nodes, it is usual to have L/S ratio less than 2 as these nodes tend to be rounded.

Mack et al also stated that “all the IMLNs had either a visible fatty hilum or a normally shaped lobular or oval appearance with circumscribed margins”; however, it is not clearly defined how many of the lymph nodes lacked fatty hilum despite normal shape. In our study, the fatty hilum was not identified in 168 nodes (65.7%). Forty-two percent of these nodes were small sized (long axis smaller than 3 mm). As the node gets larger, it was easier to identify the fatty hilum. However, for some cases despite the relatively large size of the node, the hilar notch could not be visualized due to respiratory/cardiac motion artifact or when the hilum is not parallel to the imaging plane.

In addition to high-risk patients, our study also involved other MRI indication groups such as implant imaging. These patients had the largest nodes compared with other groups (► **Table 4**). In Sutton et al's 2015 study involving 207 IMLNs among patients with breast implants who had undergone oncologic surgery, only one (0.48%) was found to be malignant.<sup>23</sup> Enlargement of the lymph nodes is thought to represent the foreign body reaction of the body to the implant.<sup>24</sup>

In 2015, Ray et al published a study that included follow-ups of incidentally found IMLNs on 320 consecutive screening breast MRI examinations in 92 women without MRI evidence of malignancy.<sup>25</sup> IMLN frequency and size were similar to Mack et al's study, being positive in 45 of 92 cases (49%) with a mean long axis of 4 mm (range: 3–10 mm). None of the patients developed breast cancer after a mean follow-up interval of 3 years (range: 1–10 years). Their study was mostly based on the size of the node and follow-up behavior rather than the morphological features. Similar to our study, none of the nodes in their study group showed significant growth during follow-ups.

In Savaridas et al's retrospective computed tomography study analyzing 149 patients who were diagnosed with primary breast cancer within the 48-month time frame, it was found that 42% ( $n=62$ ) of the cases were positive for IMLN, while the majority were small sized ( $<5$  mm).<sup>26</sup> They showed that patients with large ( $>5$  mm) IMLN either had distant metastases or additional adenopathy. In our study of benign IMLNs, the mean long axis size of the largest node of each patient was 4.57 mm and the mean long axis size of overall nodes was 3.9 mm. We know that L/S ratio is more useful rather than axis sizes alone since a node with a large size of the long axis might still be benign as long as it is elliptical with a preserved fatty hilum.

Although Lee and Kim's study had a superiority comparing benign ( $n=40$ ) and malignant ( $n=19$ ) IMLNs of 59 patients, lacking pathological results for some of the cases was a limitation.<sup>27</sup> The lymph nodes that decreased in size post-chemotherapy were included in the malignant group; however, we know that even benign vascularized/fast growing breast masses such as fibroadenomas might also decrease in size after medical treatment. The short axis size was found to be the most discriminative variable in their study with a threshold of 4 mm to predict metastases. All the 19 benign cases of the benign subgroup had fatty hilum. However, they excluded cases with a long axis less than 5 mm and defined them as too small to characterize. Our study involved all the IMLNs regardless of the size as long as it is defined as a lymph node in all the sequences with consensus. About 28.1% ( $n=72$ ) of the nodes in our study had a long axis less than 3mm. Of these, the rate of identifying fatty hilum (2.7%) was remarkably less than the larger ones. This is not surprising as the spatial resolution is limited by the pixel size. The difficulty for identifying the fatty hilum in most of our cases could be attributed to the small size of the lymph node.

Ipsilateral reactive intramammary lymph node was identified in 10% of the cases. In the literature, the prevalence of intramammary lymph nodes have been reported to vary

between 0.7 and 48%.<sup>28,29</sup> The huge variation might be caused by the retrospective method of the studies using different modalities. As the exact numbers are unclear, we were unable to describe a correlation between the incidence of intramammary lymph nodes and IMLN.

About 32.3% of the patients had a history of ipsilateral breast intervention. This is much higher than the general population. We do not know whether the IMLN was formed as a reaction to the intervention. Our study group mostly involves high-risk patients and patients for whom MRI was recommended. These patients have higher rates of being biopsied; therefore, bias is inevitable.

Our study has some limitations. First of all, only benign lymph nodes without a comparison group consisting of malignant cases were evaluated; therefore, no cutoff point for L/S ratio could be given. Number of cases with MRI indications other than high-risk screening such as implant imaging are limited. Finally, 1.5T and 3T MRI exams could not be evaluated separately and compared as patients had been scanned in different magnets throughout follow-ups.

In conclusion, like benign axillary lymph nodes, benign IMLNs can be frequently detected on breast MRIs without signs of malignancy. These nodes tend to be larger in patients with breast implants and tend to be stable over time. We believe it is not necessary to mention IMLNs smaller than 3mm in patients without suspicious breast lesions. For nodes larger than 3mm, L/S ratio and fatty hilum should be evaluated. The ones with a rounded appearance (L/S ↓) and where fatty hilum is not seen despite the large size could be evaluated more carefully and managed according to the patient's risk factors.

#### Funding

No funding.

#### Conflict of Interest

The authors declare that they have no conflict of interest.

#### Acknowledgments

None.

#### References

- 1 Alduk AM, Prutki M, Stern-Padovan R. Incidental extra-mammary findings in breast MRI. *Clin Radiol* 2015;70(05):523–527
- 2 Nelson HD, Zakher B, Cantor A, et al. Risk factors for breast cancer for women aged 40 to 49 years: a systematic review and meta-analysis. *Ann Intern Med* 2012;156(09):635–648
- 3 Cancer Care Ontario (CCO) Information for Healthcare Providers on the Ontario Breast Screening Program (OBSP) [(accessed on 15 January 2019)]; Accessed May 12, 2022 online: <https://archive.cancercare.on.ca/pcs/screening/breastscreening/OBSP/>
- 4 Smith RA, Saslow D, Sawyer KA, et al; American Cancer Society High-Risk Work Group; American Cancer Society Screening Older Women Work Group; American Cancer Society Mammography Work Group; American Cancer Society Physical Examination Work Group; American Cancer Society New Technologies Work Group; American Cancer Society Breast Cancer Advisory Group. American Cancer Society guidelines for breast cancer screening: update 2003. *CA Cancer J Clin* 2003;53(03):141–169

- 5 Lee CH, Dershaw DD, Kopans D, et al. Breast cancer screening with imaging: recommendations from the Society of Breast Imaging and the ACR on the use of mammography, breast MRI, breast ultrasound, and other technologies for the detection of clinically occult breast cancer. *J Am Coll Radiol* 2010;7(01):18–27
- 6 Warner E, Messersmith H, Causer P, Eisen A, Shumak R, Plewes D. Systematic review: using magnetic resonance imaging to screen women at high risk for breast cancer. *Ann Intern Med* 2008;148(09):671–679
- 7 Mainiero MB, Cinelli CM, Koelliker SL, Graves TA, Chung MA. Axillary ultrasound and fine-needle aspiration in the preoperative evaluation of the breast cancer patient: an algorithm based on tumor size and lymph node appearance. *AJR Am J Roentgenol* 2010;195(05):1261–1267
- 8 Uematsu T, Sano M, Homma K. In vitro high-resolution helical CT of small axillary lymph nodes in patients with breast cancer: correlation of CT and histology. *AJR Am J Roentgenol* 2001;176(04):1069–1074
- 9 Dogan BE, Dryden MJ, Wei W, et al. Sonography and sonographically guided needle biopsy of internal mammary nodes in staging of patients with breast cancer. *AJR Am J Roentgenol* 2015;205(04):905–911
- 10 Veronesi U, Paganelli G, Viale G, et al. Sentinel-lymph-node biopsy as a staging procedure in breast cancer: update of a randomised controlled study. *Lancet Oncol* 2006;7(12):983–990
- 11 Gradishar WJ, Anderson BO, Balassanian R, et al. NCCN clinical practice guidelines in oncology. *J Natl Compr Canc Netw* 2016;14(03):324–354
- 12 Wernli KJ, DeMartini WB, Ichikawa L, et al; Breast Cancer Surveillance Consortium. Patterns of breast magnetic resonance imaging use in community practice. *JAMA Intern Med* 2014;174(01):125–132
- 13 Grabau D, Jensen MB, Rank F, Blichert-Toft M. Axillary lymph node micrometastases in invasive breast cancer: national figures on incidence and overall survival. *APMIS* 2007;115(07):828–837
- 14 Sivridis E, Giatromanolaki A, Galazios G, Koukourakis MI. Node-related factors and survival in node-positive breast carcinomas. *Breast* 2006;15(03):382–389
- 15 Woo CS, Silberman H, Nakamura SK, et al. Lymph node status combined with lymphovascular invasion creates a more powerful tool for predicting outcome in patients with invasive breast cancer. *Am J Surg* 2002;184(04):337–340
- 16 Mack M, Chetlen A, Liao J. Incidental internal mammary lymph nodes visualized on screening breast MRI. *AJR Am J Roentgenol* 2015;205(01):209–214
- 17 Sachdev S, Goodman CR, Neuschler E, et al. Radiotherapy of MRI-detected involved internal mammary lymph nodes in breast cancer. *Radiat Oncol* 2017;12(01):199
- 18 Wang Y, Qi W, Xu H, et al. Infiltration tendency of internal mammary lymph nodes involvement in patients with breast cancer: anatomical characteristics and implications for target delineation. *Radiat Oncol* 2019;14(01):208
- 19 Ying M, Ahuja AT, Evans R, King W, Metreweli C. Cervical lymphadenopathy: sonographic differentiation between tuberculous nodes and nodal metastases from non-head and neck carcinomas. *J Clin Ultrasound* 1998;26(08):383–389
- 20 Sugama Y, Kitamura S. Ultrasonographic evaluation of neck and supraclavicular lymph nodes metastasized from lung cancer. *Intern Med* 1992;31(02):160–164
- 21 Yao ZH, Wu AR. [Supraclavicular lymph node metastasis from carcinoma of the uterine cervix after radiotherapy—analysis of 219 patients]. *Zhonghua Zhong Liu Za Zhi* 1988;10(03):230–232
- 22 Choi YJ, Ko EY, Han BK, Shin JH, Kang SS, Hahn SY. High-resolution ultrasonographic features of axillary lymph node metastasis in patients with breast cancer. *Breast* 2009;18(02):119–122
- 23 Sutton EJ, Watson EJ, Gibbons G, et al. Incidence of internal mammary lymph nodes with silicone breast implants at MR imaging after oncoplastic surgery. *Radiology* 2015;277(02):381–387
- 24 Zambacos GJ, Molnar C, Mandrekas AD. Silicone lymphadenopathy after breast augmentation: case reports, review of the literature, and current thoughts. *Aesthetic Plast Surg* 2013;37(02):278–289
- 25 Ray KM, Munir R, Wisner DJ, et al. Internal mammary lymph nodes as incidental findings at screening breast MRI. *Clin Imaging* 2015;39(05):791–793
- 26 Savaridas SL, Spratt JD, Cox J. Incidence and potential significance of internal mammary lymphadenopathy on computed tomography in patients with a diagnosis of primary breast cancer. *Breast Cancer (Auckl)* 2015;9:59–65
- 27 Lee HW, Kim SH. Breast magnetic resonance imaging for assessment of internal mammary lymph node status in breast cancer. *J Breast Cancer* 2016;19(02):191–198
- 28 Stomper PC, Leibowich S, Meyer JE. The prevalence and distribution of well circumscribed nodules on screening mammography: analysis of 1500 mammograms. *Breast Dis* 1991;4:197–203
- 29 Abdullgaffar B, Gopal P, Abdulrahim M, Ghazi E, Mohamed E. The significance of intramammary lymph nodes in breast cancer: a systematic review and meta-analysis. *Int J Surg Pathol* 2012;20(06):555–563